

Model analysis for combustion characteristics of RDF pellet^①

LIU Guiqing¹, H. Hakamada², Y. Itaya¹, S. Hatano¹, S. Mori¹

(1. Department of Chemical Engineering, Nagoya University, Japan;

2. Chemical & Environmental Engineering Department, Kawasaki Heavy Industries, Ltd., Japan)

[Abstract] Fundamental studies of the combustion characteristics and the de-HCl behavior of a single refuse-derived fuel (RDF) pellet were carried out to explain the de-HCl phenomena of RDF during fluidized bed combustion and to provide data for the development of high efficiency power generation technology using RDF previously. For further interpreting the devolatilization and the char combustion processes of RDF quantitatively, an unsteady combustion model for single RDF pellet, involving reaction rates, heat transfer and oxygen diffusion in the RDF pellet, was developed. Comparisons of simulation results with experimental data for mass loss of the RDF samples made from municipal solid waste, wood chips and poly-propylene when they were heated at 10K/min or put into the furnace under 1 073 K show the verifiability of the model. Using this model, the distributions of the temperature and the reaction ratio along the radius of RDF pellet during the devolatilization process and the char combustion process were presented, and discussion about the inference of heating rate on the combustion characteristics were performed.

[Key words] refuse derived fuel; combustion characteristics; de-HCl; modeling analysis

[CLC number] X 705

[Document code] A

1 INTRODUCTION

With the development of industrialization and urbanization, proper treatment and recycling utilization of wastes have become important tasks of our society. The recycling approaches of solid wastes can be classified as material recycle and energy-recovery. Although many wastes such as wood, paper and natural fiber can be recycled as material to reduce the consumption of virgin materials, since the original materials of plastics, synthetic rubber and synthetic fibers come from petroleum, thermal recycling of these wastes can not only treat the wastes effectively but also reduce the consumption of petroleum used as fuel. So the thermal recycling of wastes become an attractive approach for waste treatment and energy recovery. Among the thermal treatment technologies, use of refuse-derived fuel (RDF) as starting materials for combustion and gasification processes presents several advantages over direct use of municipal or other solid wastes. RDF is generally produced by selecting the combustible fraction of municipal solid waste (MSW) by mechanical sorting and processing. This results in a relatively constant composition and good transportation and storage possibilities, since putrescible components are eliminated with lime addition. Therefore, RDF can be produced dispersively then transported to a large-scale treatment facility to accomplish efficient energy recovery and minimization of pollution^[1]. Especially, some recent investigations have shown that de-HCl behavior of the calcium compound in the RDF during the combustion of RDF in fluidized bed can effectively control the corrosion problem caused by the

flue gas and the release of dioxins is quite low as well^[2, 3]. Tests of RDF in fluidized bed combustion (FBC) boiler have given unexpected high de-HCl efficiency (60% ~ 85%), resulting in very low concentrations of HCl (below 10^{-4}) at the inlet of baghouse even under high furnace temperature (830 ~ 850 °C)^[2, 4, 5], while the HCl removal efficiency in a stoker-type incinerator for MSW with lime injection was as low as 4% ~ 25%, resulting in very high concentration of HCl in the flue gas between 5.51×10^{-6} ~ 7.47×10^{-6} .

In our previous studies, the combustion characteristics and the de-HCl effect of a single RDF pellet have been investigated through a series of experiments carried out in an electric furnace^[6, 7]. Through these fundamental studies, it has been known that, 1) the mass loss of RDF was mainly due to devolatilization and the temperature gradient in the RDF pellet strongly depended on the heating rate and the oxygen concentration in the ambient gas^[6]; 2) calcium compounds added to RDF can capture more amount of Cl released from the RDF under quick heating condition than under the slow heating condition, and oxygen concentration of the feed gas had a strong inference on the capture of Cl by the ash. The higher the oxygen concentration was, the lower the capture fraction of Cl was^[7].

In order to provide further information on combustion characteristics and de-HCl mechanism during combustion of RDF quantitatively, in this study, an unsteady combustion model, involving reaction rate, heat transfer and oxygen diffusion in RDF pellet, is developed. Using this model, the distributions of

temperature and reaction ratio along the radius of RDF pellet during the devolatilization process and the char combustion process are predicted, and discussions about the inference of heating rate on the combustion characteristics are performed.

2 MODEL

The samples used in this study are of shape in cylinder with diameter between 1.5~2.0 cm and length between 3.0~6.0 cm. According to the results obtained in the previous study, the combustion process of RDF consists of two sequential processes: the devolatilization process and the char combustion process. So in the combustion model two-step reaction kinetics is considered. It is assumed that the char combustion begins when the overall reaction of devolatilization completes 99%. To simplify the calculation program, following assumptions are also accepted in the formulation of present model: 1) Solid spatial dimensions are considered constant; 2) As the aspect ratios of the samples are more than two, the end effects caused by the mass and heat transfer along the axis are negligible; 3) The reaction order of devolatilization is one.

Assumption 1 has been widely used in the modeling of biomass pyrolysis. In the case of RDF, it is based on the observation results obtained by pre-experiments, where no relevant shrinkage phenomena were observed. Assumption 3 has been verified with the experimental results in TG analysis using pulverized RDF sample^[4].

The model equations based on the preceding assumptions are listed as follows.

Heat balance

$$\frac{\partial^2 T}{\partial r^2} + \frac{1}{r} \frac{\partial T}{\partial r} + \frac{q}{\lambda} = \frac{1}{\alpha} \frac{\partial T}{\partial t} \quad (1)$$

Reaction heat

$$q = R(x_i(r), T(r))(-\Delta H_i) \quad (2)$$

(for devolatilization and char combustion process, $i = 1, 2$ respectively)

Mass balance:

$$\rho_s f_1 \frac{\partial x_i}{\partial t} = R(x_i(r), T(r)) \quad (3)$$

Degree of conversion:

$$x_i = \frac{w_{s0,i} - w_{s,i}}{w_{s0,i}} \quad (4)$$

Diffusion of oxygen:

$$\frac{\partial c}{\partial t} = D_e \left(\frac{\partial^2 c}{\partial r^2} + \frac{1}{r} \frac{\partial c}{\partial r} \right) + R_g(x_2(r)) \quad (5)$$

Consumption of oxygen:

$$R_g(x_2(r)) = -\frac{w_{sc0}}{2M} \frac{dx_2}{dt} \quad (6)$$

Reaction rate of devolatilization:

$$R(x_1(r), T(r)) = \frac{\rho_0}{f_1} A_1 \exp\left(-\frac{E_1}{RT(r)}\right) \cdot (1 - x_1(r)) \quad (7)$$

Reaction rate of char combustion (based on Grain Model):

$$R(x_2(r), T(r)) = A_2 \exp\left(-\frac{E_2}{RT(r)}\right) \cdot C^n(r) (1 - x_2(r))^{2/3} \quad (8)$$

3 EXPERIMENT AND DETERMINATION OF PHYSICAL PROPERTIES AND MODEL PARAMETERS

3.1 Combustion experiment

An electric heating reactor was used for combustion experiments on single RDF pellets. The experimental system was fully described previously^[6], so only the essential features were given herein. The reactor was constructed by connecting a vertical quartz tube (53 mm in diameter, 1 000 mm in length) working as primary reactor and a horizontal quartz tube (45 mm in diameter, 300 mm in length) working as secondary combustion chamber. Two separated electric heaters with PID controllers were used to maintain the temperatures of two combustion chambers independently. A quartz pan used as sample supporter was hung on a digital electric balance with a long-thin Inconel alloy wire. When the experimental system was set to measure the temperatures in the RDF pellet, the sample supporting system was replaced by a thin quartz pipe including the probes of thermocouples. Purge gas was supplied from the bottom to maintain the oxygen concentration constant during each run. The oxygen concentration in the purge gas was regulated from 0 to 21% by changing the mixing ratio between pure nitrogen and air. The total flow rate of the purge gas was kept constant at 5×10^{-2} m³/min (at 298 K and 101 kPa) during all runs. Pure oxygen (> 90%) was used as secondary air to promote the burn-out of organic substances in the flue gas in the secondary chamber.

3.2 RDF samples and chemical properties

Experimental runs were performed with three kinds of RDF: a commercial RDF made from MSW, a model RDF made of wood chip and polypropylene pellet. Their chemical features are given in Table 1.

3.3 Physical properties and model parameters

The necessary physical properties and model parameters were determined through pre-experimental works. The thermal conductivities of RDF (λ_0) and their char (λ_c) were measured with a Thermal Conductivity Meter in room temperature, then the values were calibrated for the operating temperature with the Kunii & Smith Equation. The thermal conductivity for the sample during the devolatilization and char combustion process was evaluated according to a proportional relation between the thermal conductiv-

ty and the density of the sample.

The reaction heat ($-\Delta H_i$) and the specific heat capacity (C_p) of RDF were measured by means of differential scanning calorimeter (DSC). The data presented in Refs. [8, 9] were adopted for the specific heat capacities of char and volatiles.

The activation energy (E_1) and the pre-exponential factor (A_1) for the devolatilization were obtained through TG analysis by using of the sample pulverized from RDF under an inert atmosphere^[4], and the activation energy (E_2) and the pre-exponential factor (A_2) for the char combustion were determined by TGA under different oxygen concentrations using pulverized char sample obtained by pyrolysis experiment under 1 073 K^[11].

The effective diffusion coefficient of the oxygen was evaluated by the method presented in Ref. [12].

The physical properties and the model parameters obtained are given in Table 2 and Table 3, respectively.

4 RESULTS AND DISCUSSION

4.1 Comparison between experimental data and calculation results for mass loss curve

The calculation results by present model and the experimental results for RDF-m are shown in Fig. 1. In the case of slow heating (10 K/min) in air ($C_A = 21\%$), as shown in Fig. 1(a), excepting the results for the initial period of the process, the mass loss curves are well agreeable in the overall process. The difference that occurred in the initial period is believed to be the result of the vaporization of moisture in the sample.

Table 1 Properties of tested RDF (Dry base except for moisture)

| Sample | Higher heating value / (kJ·kg ⁻¹) | Proximate analysis/ % | | | | Ultimate analysis/ % | | | | | | Pellet density / (kg·m ⁻³) | |
|--------|---|------------------------|----------|--------------|------|----------------------|------|------|-------|------|--------|--|-------|
| | | Moisture (as received) | Volatile | Fixed carbon | Ash | C | H | N | O | S | Cl | Ca | |
| RDF-wd | 20 110 | 8.1 | 81.2 | 17.8 | 1.0 | 45.2 | 5.5 | 0.9 | 47.4 | 0.02 | Trace | < 0.1 | 1 540 |
| RDF-pp | 45 850 | < 0.1 | 99.3 | 0.1 | 0.6 | 84.4 | 15.0 | 0.34 | < 0.1 | 0.01 | < 0.01 | 3.0 | 1 540 |
| RDF-m | 15 280 | 6.3 | 69.5 | 10.1 | 20.4 | 35.2 | 6.0 | 0.7 | 32.3 | 0.10 | 1.20 | 9.2 | 1 560 |

Table 2 Physical properties of RDFs

| Sample | | Diameter / cm | Density, $w_i / (\text{kg} \cdot \text{m}^{-3})$ | Thermal conductivity, $\lambda / (\text{W} \cdot \text{m}^{-1} \cdot \text{K}^{-1})$ | Specific heat capacity, $c_p / (\text{J} \cdot \text{kg}^{-1} \cdot \text{K}^{-1})$ | Diffusion coefficient, $D_e / (\text{m}^2 \cdot \text{s}^{-1})$ |
|----------|------|---------------|--|--|---|---|
| RDF-m | RDF | 2.0 | 1 154 | 0.29 | $1 097 + 3.44 \times 10^{-2} T$ | — |
| | Char | 1.6 | 698 | 0.10 | $1 003 + 2.09 T^{[10]}$ | — |
| | Ash | — | 581 | 0.06 | — | 8.0×10^{-6} |
| RDF-wd | RDF | 1.6 | 1 045 | 0.20 | $1 320 + 3.44 \times 10^{-2} T$ | — |
| | Char | 1.3 | 360 | 0.10 | $1 003 + 2.09 T^{[10]}$ | — |
| | Ash | — | 12 | 0.06 | — | 1.6×10^{-5} |
| RDF-pp | RDF | 1.0 | 1 540 | 0.20 | 2 000 | — |
| Volatile | | — | — | $4.2 \times 10^{-2} + 3.8 \times 10^{-4} T - 7 \times 10^{-8} T^2 [12]$ | $1 100^{[11]}$ | — |

Table 3 Kinetic parameters for devolatilization and char combustion of RDFs

| Sample | Devolatilization | | | | Char combustion | | | |
|--------|--|---|----------------|--|--|---|----------------|--|
| | Pre-exponential factor / s ⁻¹ | Activation energy / (kJ·mol ⁻¹) | Reaction order | Heat of reaction / (kJ·mol ⁻¹) | Pre-exponential factor / s ⁻¹ | Activation energy / (kJ·mol ⁻¹) | Reaction order | Heat of reaction / (kJ·mol ⁻¹) |
| RDF-m | 1.7×10^3 | 62.0 | 1 | 1.0×10^{-2} | 3.1×10^4 | 20.0 | 1 | 22.4×10^3 |
| RDF-wd | 7.0×10^4 | 72.0 | 1 | 1.0×10^{-3} | 3.1×10^4 | 20.0 | 1 | 20.0×10^3 |
| RDF-pp | 6.3×10^9 | 140.1 | 1 | 1.0×10^{-2} | | | | |

In the case of quick heating where the sample was inserted to the isothermal atmosphere (1 073 K) shown in Fig. 1 (b), the results are well consistent throughout the devolatilization process. But little deviation presented in the char combustion process of RDF-m and RDF-wd. This phenomenon is a reflection of the complexity for reaction during char combustion process. By the comparisons, the reliability of the model calculation is verified.

4.2 Model prediction of temperature and reaction distribution for RDF-m

4.2.1 In case of slow heating at heating rate of 10 K/min in air

The calculation results for the temperature distribution and the reaction ratio of RDF-m with time are shown in Fig. 2.

During the devolatilization process (as shown in Fig. 2(a)), the temperature increases with heating time almost evenly along the radial direction, while

the progress of reaction is homogeneous within the RDF and accelerated with heating time. During the char combustion process (as shown in Fig. 2(b)), with the progress of reaction, a peak temperature is shifted from the surface to center along the radial direction. From the reaction ratio curves it is found that there exists a clear boundary between reacted part and unreacted part along the radius, indicating that the reaction occurs on the surface of a shrinking unreacted core.

4.2.2 In case of isothermal condition at 1 073 K

When the sample was inserted to the hot zone ($T = 1 073$ K, $C_A = 10\%$) of the furnace instantaneously, it was heated quickly from the surface to the center. The temperature distribution and the reaction ratio of RDF-m with time are shown in Fig. 3.

The features both for the temperature and reaction ratio distribution during the devolatilization process are obviously different from that in slow heating case. While the temperature close to the surface of

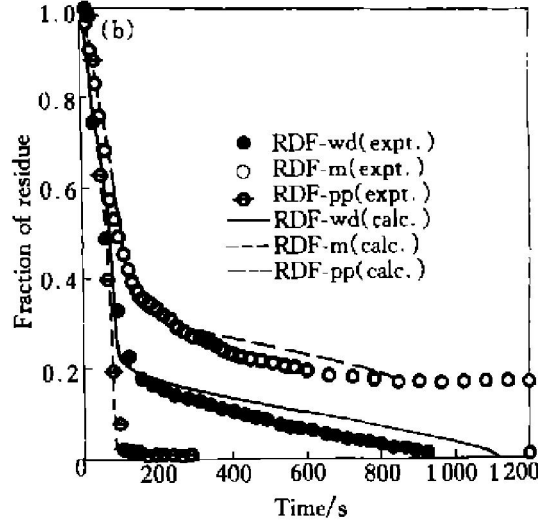
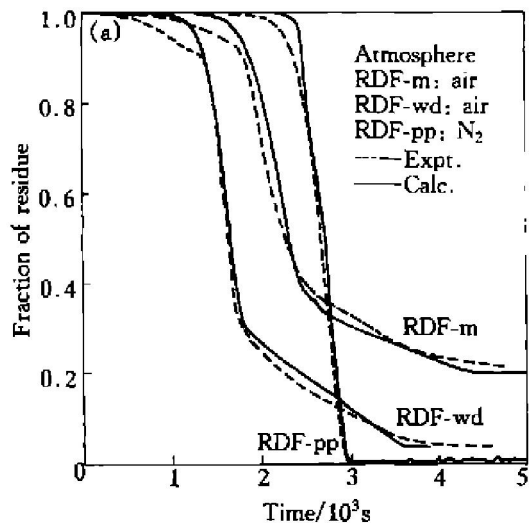


Fig. 1 Comparison of calculated results with experimental data
(a) —Slow heating (heating rate = 10 K/min); (b) —Isothermal heating (furnace temperature = 1 073 K)

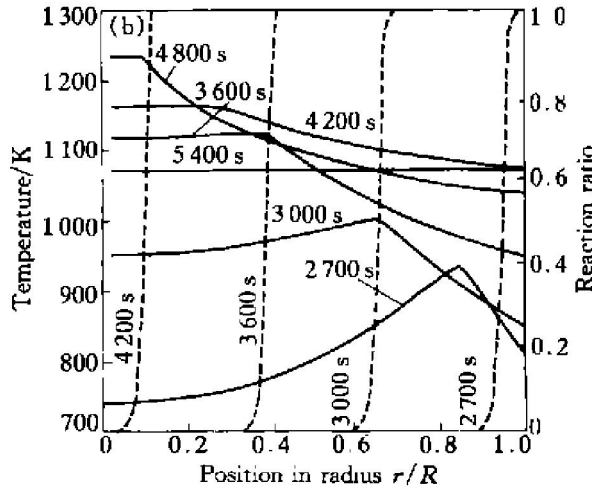
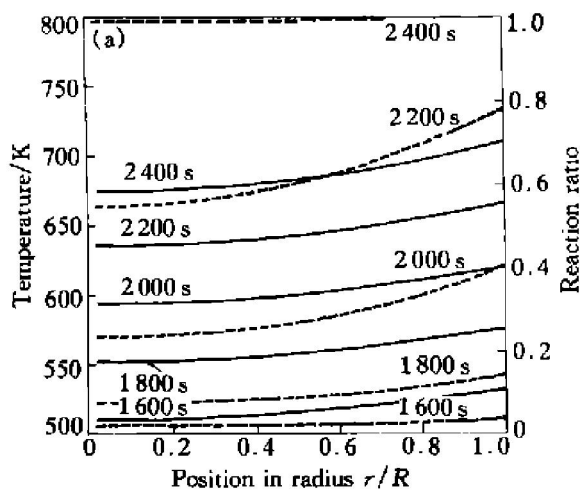


Fig. 2 Temperature and reaction ratio distribution in RDF-m heated at 10 K/min in air
(a) —Devolatilization process; (b) —Char combustion process
— Temperature; - - - Reaction ratio

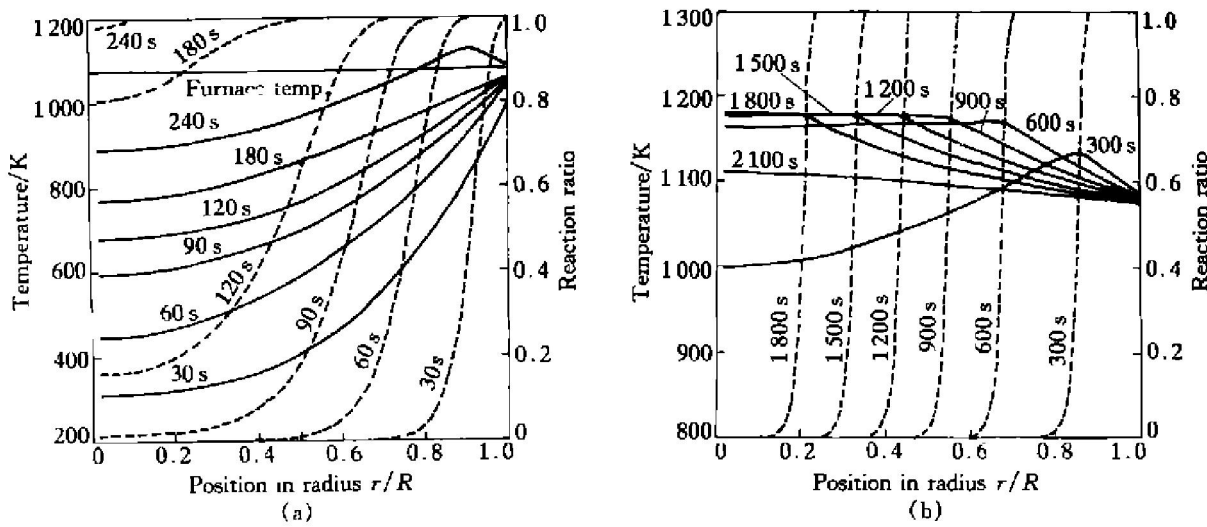


Fig. 3 Temperature and reaction ratio distribution in RDF-m inserted in furnace at 1073 K, $C_A = 10\%$

(a) — Devolatilization process; (b) — Char combustion process
— Temperature; - - - Reaction ratio

RDF is increased dramatically to near the furnace temperature, the temperature inside the RDF keeps quite low. Therefore, a significant temperature gradient forms along the radius at first and then fades with time. A reaction boundary is formed in the early period, but it disappears gradually accompanying the fading of temperature gradient. This phenomenon indicates that the reaction is shifted from thermal transfer controlled process to chemical reaction controlled process.

During the char combustion process, the features of temperature and reaction ratio are similar to those in the case of slow heating, where a clear boundary exists between reacted part and unreacted part along the radius, and the reaction occurs on the surface of a shrinking unreacted core. However, the temperature peak inside the RDF is not so sharp as in the case of slow heating. This is attributed to the moderate combustion in low oxygen concentration atmosphere. Therefore, the char combustion rate seems to be controlled by the diffusion of oxygen through the reacted layer.

5 CONCLUSION

The quite good agreement between the results of model calculations and the experimental data shows that the model presented herein is a viable tool for the quantitative description of the overall combustion process of RDF pellet.

The results of model calculations for the distribution of temperature and reaction ratio in the RDF indicate that the heating rate is an important parameter during the devolatilization of RDF, where the process can be changed from reaction rate controlling to thermal conductivity controlling as the heating rate in-

creases.

The results also show that char combustion process is not influenced by the heating rate. During char combustion, it keeps a clear boundary between the reacted part and unreacted part along the radial direction, so a shrinking unreacted core is formed, and combustion seems to be controlled by the diffusion of oxygen through the reacted layer.

Nomenclature

- c — Concentration of oxygen in the char, mol/m³;
- C_A — Volume fraction of oxygen in purge gas, %;
- D_e — Effective diffusion coefficient, m²/s;
- f_1 — Fraction of volatile;
- M — Average molecular mass of combustible component in char, g/mol;
- q — Heat generated unit volume, W/m³;
- R — Radius of RDF pellet, m;
- R_g — Oxygen consumption rate, mol/(m³•s);
- r — Radial distance of RDF pellet, m;
- T, T_c, T_s — Temperature parameter, K;
- t — Time, s;
- $w_{s,i}$ — Concentration of reactants in solid, kg/m³;
- $w_{s0,i}$ — Initial concentration of reactants in solid, kg/m³;
- w_{sc0} — Initial concentration of reactants in char, kg/m³;
- x, x_i, x_1, x_2 — Reaction ratio;
- α — Thermal diffusivity, m²/s;
- $\lambda, \lambda_0, \lambda_c$ — Apparent heat conductivity, W/(m•K);
- ρ_0 — Apparent density of RDF, kg/m³;

ρ_s —Apparent density of solid, kg/m³;

Subscripts:

0—Initial

1—Devolatilization process

2—Char combustion process

c—Center at cross section of RDF

s—Surface on the wall of RDF

calc. —Calculation value

expt. —Experimental value

Acknowledgement

This study was partially supported by the JSPS grant for Research for the Future Program (No. 97I00604) and this presentation was partially supported by the Grant-in-Aid for International Exchange from Research Foundation for the Electrotechnology of Chubu.

[REFERENCES]

- [1] Kagiya T. Practical use and future topics concerning RDF technology for municipal solid waste management [J]. Haikibutsu Gakkaishi, 1996, 7: 352– 362.
- [2] Sugiyama H, Kagawa S, Kamiya H, et al. Chlorine behavior in fluidized bed incineration of refuse-derived fuels [J]. Environmental Engineering Science, 1998, 15: 97 – 105.
- [3] Kondoh M, Hamai M, Yamaguchi M, et al. Dioxin e-

mission with the combustion of RDF in an inner cycling fluidized bed [J]. Kagaku Kogaku Ronbunshu, 1999, 25: 921– 927.

- [4] Narukawa K, Chen Y, Yamazaki R, et al. Combustion characteristics of RDF [J]. Kagaku Kogaku Ronbunshu, 1996, 22: 1408– 1414.
- [5] Mori S. Gomi kokeika nenryo hatsuden system [J]. Nenryo & Nensho, 1996, 63: 563– 570.
- [6] Liu G, Yamazaki R, Hatano S, et al. Combustion characteristics of single cylindrical RDF [J]. Kagaku Kogaku Ronbunshu, 1999, 25: 79– 84.
- [7] Liu G, Itaya Y, Yamazaki R, et al. Behavior of chlorine during the combustion of single RDF pellet [J]. Kagaku Kogaku Ronbunshu, 2001, 27: 100– 105.
- [8] Koufopanos C A, Maschio G, Lucchesi A. Kinetic modeling of the pyrolysis of biomass and biomass components [J]. The Canadian Journal of Chemical Engineering, 1989, 67: 75– 84.
- [9] Di Blasi C. Analysis of convection and secondary reaction effects within porous solid fuels undergoing pyrolysis [J]. Combust Sci Tech, 1993, 90: 315.
- [10] Perry R H, Green D W. Perry's Chemical Engineers' Handbook [M]. New York: McGraw-Hill, 1984. 10 – 15.
- [11] Hakamada K, Liu G, Itaya Y, et al. Model analysis for pyrolysis and char combustion of RDF [A]. Proceedings of Autumn Conference of SCEJ [C]. Kanazawa, Japan, 1999.
- [12] Sato I. Bussei Josu Suisanho [M]. Maruzen, Tokyo, Japan, 1965. 129– 138.

(Edited by YUAN Sai-qian)